

Distinctive crypt shape in a sessile serrated adenoma/polyp: Distribution of Ki67-, p16^{INK4a}-, WNT5A-positive cells and intraepithelial lymphocytes

KENJI HISAMATSU^{1*}, KEI NOGUCHI^{1*}, HIROYUKI TOMITA¹, AOI MUTO¹, NATSUMI YAMADA¹, KAZUHIRO KOBAYASHI^{1,2}, AKIHIRO HIRATA³, TOMOHIRO KANAYAMA¹, AYUMI NIWA¹, KAZUHISA ISHIDA¹, TAKAYUKI NAKASHIMA¹, YUICHIRO HATANO¹, NATSUKO SUZUI², TATSUHIKO MIYAZAKI² and AKIRA HARA^{1,2}

¹Department of Tumor Pathology, Gifu University Graduate School of Medicine;

²Pathology Division, Gifu University Hospital; ³Division of Animal Experiment, Life Science Research Center, Gifu University, Gifu 501-1194, Japan

Received March 2, 2017; Accepted June 6, 2017

DOI: 10.3892/or.2017.5725

Abstract. Serrated lesions in the colorectum are currently predominantly classified as hyperplastic polyps (HPs), sessile serrated adenomas/polyps (SSA/Ps), and traditional serrated adenomas (TSAs) according to their morphology. However, the histological morphology and the molecular changes in the serrated lesions are still unclear. We performed immunohistochemistry for Ki67, p16^{INK4a}, and WNT5A in human HPs (n=22), SSA/Ps (n=41), and TSAs (n=19). The distribution of Ki67 and p16^{INK4a} positive cells in TSAs was different from that in HPs and SSA/Ps. Co-expression of Ki67 and P16^{INK4a} was infrequent in HPs and SSA/Ps; p16^{INK4a}-positive cells were found in the crypt cleft and stromal WNT5A-positive stromal cells were localized near the cleft in SSA/Ps, while intraepithelial lymphocytes (IELs) in SSA/Ps were more abundant than HPs. In conclusion, our study provides evidence that HPs branch because of the increase in and patchy distribution of senescent and proliferative cells, with increased and misdistributed stromal and inflammatory cells, which might contribute to creation of L- and/or T-shaped crypts, which are of distinctive shapes in SSA/Ps. Our findings may facilitate better understanding and therapy in the serrated lesions.

Introduction

Serrated lesions in the colorectum are characterized morphologically by elongated crypts and a saw-toothed pattern of the

crypt epithelium. The lesions are classified into hyperplastic polyps (HPs), sessile serrated adenomas/polyps (SSA/Ps), and traditional serrated adenomas (TSAs) by the World Health Organization (WHO) (1,2). These serrated lesions are similar not only in morphological appearance, but also in terms of molecular features, such as genetic and epigenetic changes (3-7). These molecular changes are found even in HPs (4,6,8), and the sequence of transformation from HPs to SSA/Ps has been thought to be premalignant. On the other hand, SSA/P diagnostic criteria, debated by many researchers, are fundamentally based on morphology in hematoxylin and eosin (HE) sections (9,10). Thus, the categorization of serrated precursor lesions, particularly HPs and SSA/Ps, still often varies among pathologists. The HP-SSA/P sequence is predominantly observed in the right-sided colon, which is different from the classical adenoma-carcinoma sequence (11). In contrast, TSAs are frequently found in the left side of colon (12), suggesting that their pathogenesis may differ from that of SSA/Ps.

p16^{INK4a} (p16), a cyclin-dependent kinase inhibitor, is a component of the INK4 family, which induces cellular senescence and growth arrest (13-15). The upregulation of p16 expression in premalignant lesions and its inactivation during malignant transformation is believed to be a common event in carcinogenesis in many organs (16,17). The loss of p16 expression caused by *CDKN2A* promoter hypermethylation contributes to malignant transformation in the serrated dysplasia-carcinoma sequence (18). However, it is not yet known whether the upregulation of p16 is linked to the serrated precursor lesions in the microscopic morphology.

In the differentiation between HP and SSA/P, some studies have suggested that a change in the Ki67-positive proliferative zone and asymmetrical change cause an architectural disturbance (9,19). Another study has demonstrated that upregulation of p16 due to oncogene-induced senescence in the premalignant serrated lesions occurs prior to a loss of p16 in malignant transformation (18), indicating that cellular proliferation and/or senescence may involve morphological

Correspondence to: Professor Hiroyuki Tomita, Department of Tumor Pathology, Gifu University Graduate School of Medicine, 1-1 Yanagido, Gifu 501-1194, Japan
E-mail: h_tomita@gifu-u.ac.jp

*Contributed equally

Key words: sessile serrated adenoma/polyp, Ki67, p16^{INK4a}, WNT5A

changes; however, the association with the localization of these molecular markers has not yet been specified.

In terms of crypt branching and fission, a recent study has revealed that Wnt5a is a key molecule in the process of crypt regeneration, particularly in crypt fission of a mouse model (20). In the mouse intestine, Wnt5a is secreted by stromal pericrypt myofibroblasts and is necessary for proliferation and branching of crypt epithelium and maintaining of homeostasis (21,22). Additionally, dysplasia branching from SSA/Ps has been reported to be closely associated with a high rate of intraepithelial lymphocytes (IELs) (23). However, the localization and role of WNT5A and IELs in the HP-SSA/P sequence are unknown.

The aim of this study was to clarify the morphological differences between SSA/P and other serrated lesions by analyzing immunohistochemistry (IHC) of Ki67 cellular proliferation marker and p16 senescence marker and furthermore, to investigate the involvement of WNT5A and IELs in the mechanism underlying development of serrated lesions, particularly SSA/Ps.

Materials and methods

Ethics statement. Human samples were obtained from Gifu University Hospital, and written informed consent was obtained from all individuals. This study was approved by the Institutional Review Board of Gifu University. All experiments were carried out in accordance with the approved guidelines of Gifu University.

Samples. Eighty-eight serrated colorectal polyps were resected endoscopically or surgically from 65 patients (aged 36 to 87 years) at the Gifu University Hospital, between the years 2012 and 2016 (Table I). The number of the polyps examined is HPs, n=22 (endoscopically, n=21; surgically, n=1), SSA/Ps, n=42 (endoscopically, n=33; surgically, n=9), and TSAs, n=24 (endoscopically, n=19; surgically, n=5).

Histological evaluation and immunohistochemistry (IHC). The histological diagnosis of the serrated lesions was evaluated based on their morphology in hematoxylin and eosin (H&E) staining (Fig. 1A). SSA/Ps were distinguished from conventional HPs on the basis of the following microscopic features: 1) crypt dilation, 2) irregularly branching crypts, and 3) horizontally arranged basal area of the crypts (inverted T- and/or L-shaped crypts) (9) (Fig. 1B). Lesions demonstrating ≥ 2 of these findings were classified as SSA/Ps. Lesions that had none of these findings were classified as HPs. TSAs were diagnosed by a complex villous architecture, lined by columnar cells with densely eosinophilic cytoplasm and pencillate nuclei (2).

All samples analyzed were formalin-fixed and paraffin-embedded tissue sections. Immunohistochemistry (IHC) was performed using a Histofine® Simple Stain MAX PO kit (Nichirei, Tokyo, Japan) according to the manufacturer's protocol. We used anti-Ki67 (mouse monoclonal antibody, clone MIB-1, 1:100 dilution; Dako Corp., Carpinteria, CA, USA), rabbit polyclonal antibody, clone SP6, 1:100 dilution; Abcam, Cambridge, MA, USA), anti-p16 (mouse monoclonal antibody, clone E6H4, 1:1 dilution; Ventana, Tucson, AZ,

USA), and anti-Wnt5a/b (rabbit monoclonal antibody, clone C27E8, 1:50 dilution; Cell Signaling, Danvers, MA, USA). For double-staining IHC, both Ki67 and p16 antibodies were used as primary antibodies. Signal amplification was performed with alkaline phosphatase-biotin complex, followed by a chromogenic reaction with alkaline phosphatase substrate kit (Vecta Blue; Vector Laboratories, Burlingame, CA, USA) and DAB as previously described (24).

To evaluate the Ki67- and p16-positive index, two representative adjacent crypts detected from the bottom to the surface of the crypt were selected in each specimen. The percentage of Ki67- or p16-expressing cells per crypt was calculated in upper, middle, and lower parts of crypt, separately (Fig. 2B). To evaluate the Wnt5a-positive index, approximately 50 to 200 crypts were selected in each specimen and the number of positive cells per crypt was calculated in the upper, middle, and lower parts of the crypt, separately. The upper portion was subdivided into the 'upper surface' (cells adjoining the surface epithelium) and 'upper else' sections (Fig. 2B). Counting of IELs in the crypt epithelium was performed in H&E sections. The number of IELs in a crypt of HPs and SSA/Ps was counted in a single hot-spot high-power field. We excluded the specimens which were not suitable for the evaluation in each examination. Histological evaluation was performed by two experienced pathologists (H.T. and K. H.) who were blinded to the clinical data.

Statistical analysis. The data were analyzed using the t-test, Fisher's exact test, and Wilcoxon's rank-sum test. $P < 0.05$ or $P < 0.01$ were considered statistically significant.

Results

Clinical characteristics. The clinical characteristics of the patients are summarized in Table I. No significant differences in sex and endoscopic morphology were found between the HP, SSA/P, and TSA groups. However, the mean age of patients with TSAs (70.9 ± 8.22 years) was significantly older than that of patients with HPs (63.8 ± 12.1 years). SSA/Ps were predominantly observed in the proximal colon (61.90%), while TSAs were found in the distal colon (70.83%); the difference in location between SSA/P and TSA was statistically significant. The mean size of HPs (7.36 ± 5.65 mm) was significantly smaller than that of SSA/Ps and TSAs (11.1 ± 6.58 and 12.7 ± 11.0 mm, respectively).

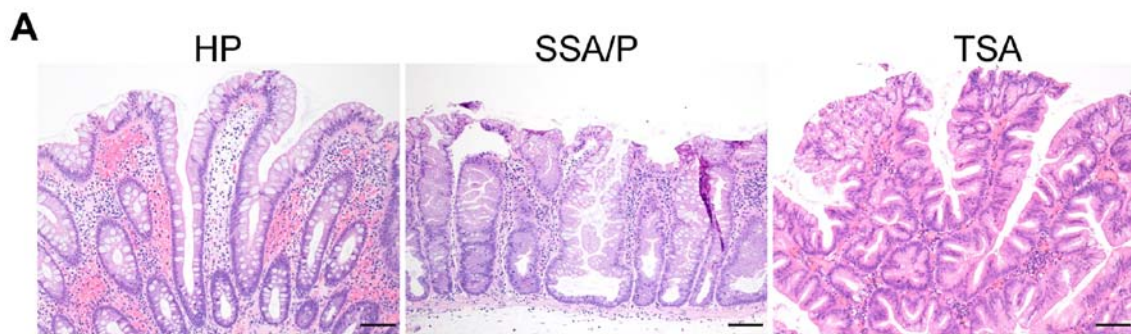
Ki67 proliferative cells expand from the lower to the middle zone in the HP-SSA/P sequence, but not in TSAs. To investigate whether morphological changes in serrated lesions are associated with cellular proliferation, we performed IHC for Ki67 in human HPs (n=22), SSA/Ps (n=41), and TSAs (n=19). In HPs and SSA/Ps, Ki67-positive cells were predominantly found in the lower third of the crypt (Fig. 2A). In TSAs, Ki67-positive cells were also observed in the lower third of the crypt; however, these cells broadly expanded toward the upper part of the crypt in TSAs in comparison with HPs and SSA/Ps.

To clarify the difference in proliferative activity between HPs, SSA/Ps, and TSAs, we calculated the Ki67-positive rate by dividing a crypt into three zones, i.e., lower, middle, and upper zones (Fig. 2B). In normal colon epithelium, the proliferative

Table I. Clinical characteristics of serrated lesions.

| Characteristics | HP (n=22) | SSA/P (n=42) | TSA (n=24) | P-value |
|------------------------------|-------------|--------------|-------------|-----------------------------------|
| Age, years | | | | 0.037 (HP vs. TSA) ^a |
| Mean ± SD | 63.8±12.1 | 68.8±10.5 | 70.9±8.22 | |
| Sex, n (%) | | | | NS |
| Male | 13 (59.09%) | 30 (71.43%) | 16 (66.67%) | |
| Female | 9 (40.91%) | 12 (28.57%) | 8 (33.33%) | |
| Location, n (%) | | | | 0.02 (SSA/P vs. TSA) ^b |
| Right colon | 11 (50.00%) | 26 (61.90%) | 7 (29.17%) | |
| Left colon | 11 (50.00%) | 16 (38.10%) | 17 (70.83%) | |
| Diameter, mm | | | | 0.004 (HP vs. SSA/P) ^a |
| Mean ± SD | 7.36±5.65 | 11.1±6.58 | 12.7±11.0 | 0.026 (HP vs. TSA) ^a |
| Endoscopic morphology, n (%) | | | | NS |
| Is | 11 (50.00%) | 14 (33.33%) | 11 (45.83%) | |
| Isp | 3 (13.64%) | 4 (9.52%) | 2 (8.33%) | |
| Ip | 0 (0.00%) | 1 (2.38%) | 3 (12.50%) | |
| IIa | 8 (36.36%) | 20 (47.62%) | 3 (12.50%) | |
| Is+IIa | 0 (0.00%) | 2 (4.76%) | 1 (4.17%) | |
| UN | 0 (0.00%) | 1 (2.38%) | 4 (16.67%) | |

NS, not significant. ^aWilcoxon's rank-sum test, ^bFisher's exact test.



B

| Diagnostic criteria of SSA/P from WHO classification (2010) |
|---|
| 1. Crypt dilation |
| 2. Irregular branching crypts (inverted T- and/or L-shaped crypts) |
| 3. Excess serration at the base of crypts |
| If straight crypt (HP-like) account for less than half of the lesion and more than two of three contiguous crypts demonstrate feature of SSA/P (1-3 in upper list), the lesion should be classified as SSA/P. |

Figure 1. Serrated lesions in the colorectum. (A) Representative images of HP, SSA/P and TSA in hematoxylin and eosin (H&E) staining. HP, hyperplastic polyp; SSA/P, sessile serrated adenoma/polyp; TSA, traditional serrated polyp (scale bars: 100 μ m). (B) Diagnostic criteria for SSA/P in the 2010 WHO classification.

zone, marked by Ki67-positive cells, is localized in the lower third of the crypt (data not shown). In HPs, SSA/Ps, and TSAs, the Ki67-positive rates were high in the lower zone of the crypt (Fig. 2C). In HPs, Ki67-positive rates in the lower, middle, and upper zones of the crypt decreased significantly (46.06, 20.62, and 2.63%, respectively). In SSA/Ps, Ki67-positive rates in the lower, middle, and upper zones of the crypt also decreased significantly (46.1, 14.31, and 1.70%, respectively). Similarly, in TSAs, the Ki67-positive rates in the lower, middle, and

upper zones of the crypt decreased significantly (36.99, 18.78, and 8.44%, respectively).

Next, we evaluated the differences in the proliferation rates between the zones in serrated lesions. In the upper zone, the proliferation rate of TSAs was significantly higher than that in HPs and SSA/Ps (Fig. 2D). In the middle zone, the proliferation rate of HPs was significantly higher than that of SSA/Ps. In the lower zone, the proliferation rates of HPs and SSA/Ps were significantly higher than that of TSAs. In the whole crypt,

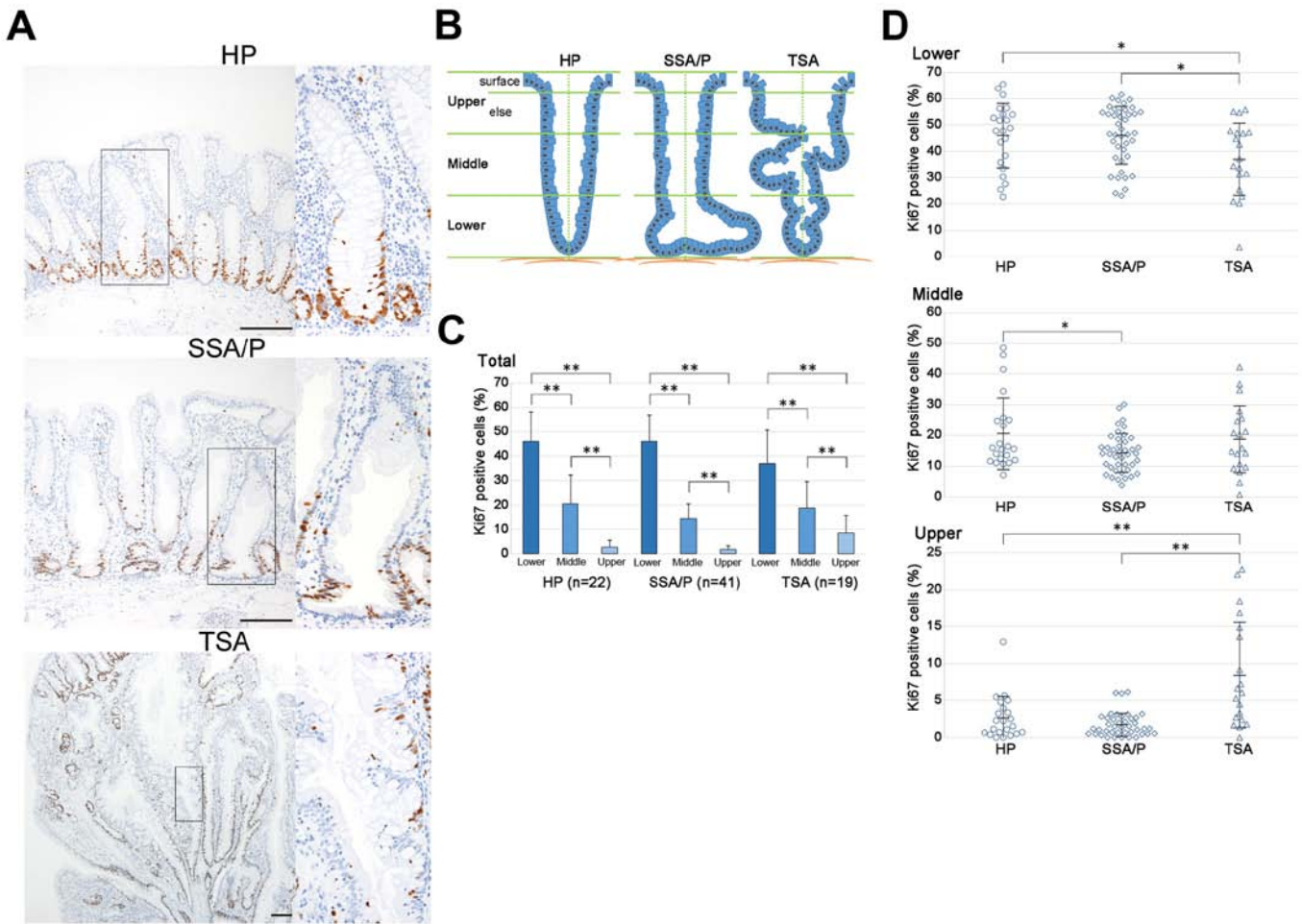


Figure 2. Ki67 expression in HP, SSA/P, and TSA. (A) Representative images of immunohistochemical expression of Ki67 in serrated lesions (scale bars: 200 μ m). (B) Evaluation by dividing a crypt into lower, middle, and upper zones. The upper zone is subdivided into 'upper surface' and 'upper else'. (C and D) Ki67-labeling index in HP, SSA/P, and TSA, in the whole (C) and individual parts (D). The central line is the arithmetic mean; error bars are \pm SD. (* P <0.05; ** P <0.01, TSA, lower vs. middle in C and lower, HP vs. TSA in D are t-test. Others are Wilcoxon's rank-sum test). HP, hyperplastic polyp; SSA/P, sessile serrated adenoma/polyp; TSA, traditional serrated polyp.

i.e. the lower, middle, and upper zones, there was no significant difference in the proliferation rates of HPs, SSA/Ps, and TSAs (23.37, 22.92, and 22.57%, respectively). These data demonstrated that the proliferative cells of SSA/Ps expanded from the lower to the middle zone, although the rate of proliferative cells was not significantly different between HPs and SSA/Ps. Furthermore, the proliferative cells of TSAs expanded broadly to all three zones and were less frequently found in the lower zone in TSAs than in those of HPs and SSA/Ps. These results suggest that there might be a marked difference in the proliferation and senescence of cells in the crypt.

Significant increase of p16 expression in the crypt bottom of SSA/Ps. To clarify whether cellular senescence is associated with serrated lesions, we performed IHC for p16, the key enforcer of cell cycle arrest, in our cohort (HPs, $n=18$; SSA/Ps, $n=28$; TSAs, $n=13$). Few p16-positive cells were observed in the normal colon epithelium (data not shown) and HPs (Fig. 3A). In several HP cases, p16-positive cells were observed in the crypt bottom. In SSA/Ps, p16-positive cells were predominantly found in the bottom of the crypt, in particular in L- or T-shaped crypts, albeit sparsely. Furthermore, p16-positive cells were

found in the cleft of the crypt. Except for the epithelium, a few stromal cells, such as lymphocytes and granulocytes, around the crypt showed positive staining. In TSAs, p16-positive epithelial cells broadly expanded across the crypt, although there were few positive cells.

Next, we evaluated differences between the rates of p16-positive senescent cells among the three zones in serrated lesions, in a similar manner as for the calculation of Ki67-positive cells. In HPs, SSA/Ps, and TSAs, the p16-positive rate of the lower zone was significantly higher than that of the upper and middle zones (Fig. 3B). In HPs, p16-positive rates in the lower, middle, and upper zones of the crypt decreased significantly (3.09, 1.02, and 0.37%, respectively). Similarly, p16-positive rates decreased significantly in SSA/P (12.76, 4.12, and 0.93%, respectively) and in TSA (17.41, 12.45, and 6.11%, respectively) in the lower, middle, and upper zones of the crypt. Consequently, the rate of the p16-positive cells followed the same trend as the Ki67-positive cells (Fig. 2C) in the crypts of serrated lesions.

We evaluated the differences in the p16-positive senescent cell rates between the crypt zones in serrated lesions. In the upper zone, the rate of the senescent cells in TSAs was significantly higher than those in HPs and SSA/Ps (Fig. 3C). In the

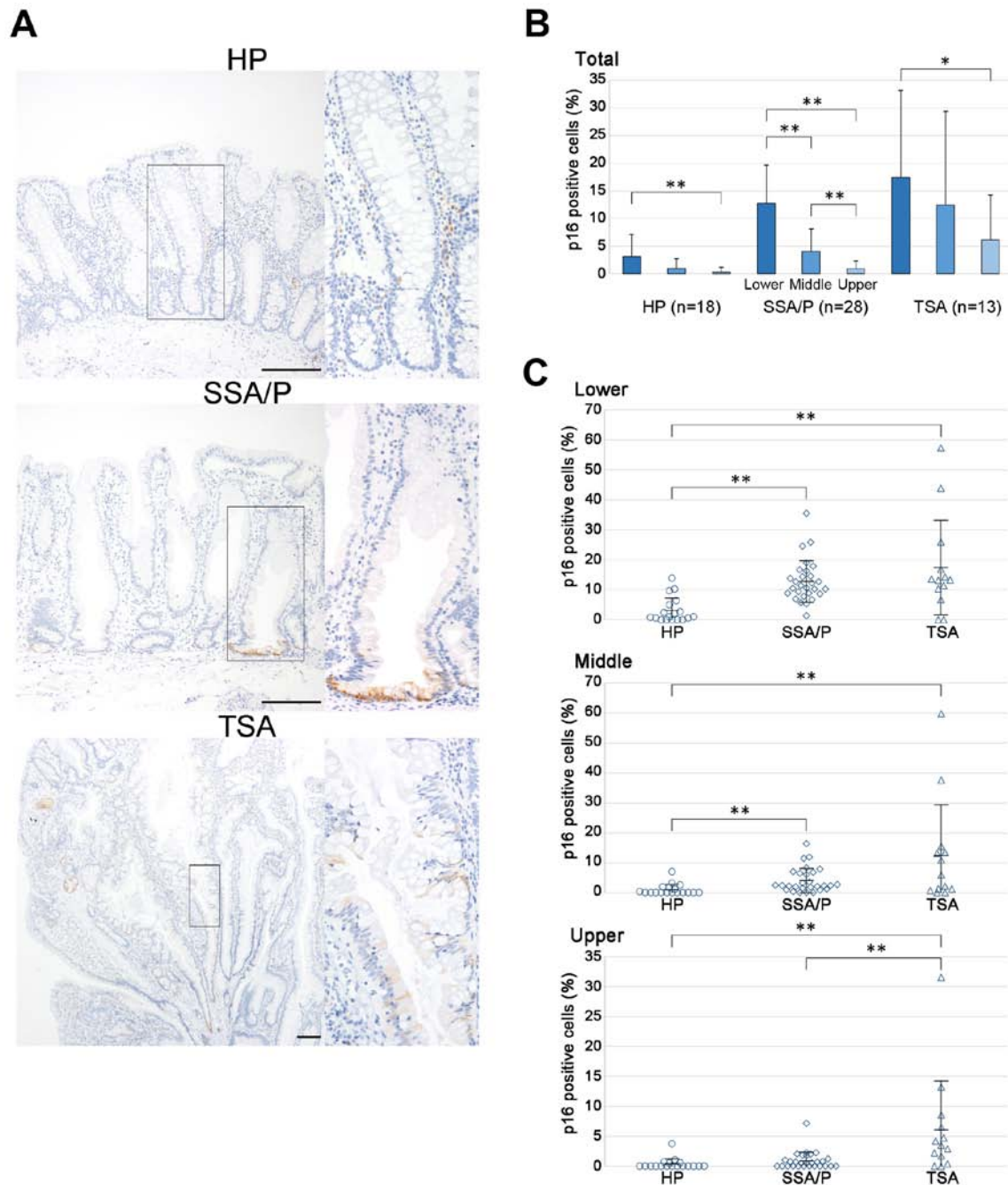


Figure 3. p16^{INK4a} expression in HP, SSA/P, and TSA. (A) Representative images of immunohistochemical expression of p16 in serrated lesions (scale bars: 200 μ m). (B and C) p16^{INK4a} positive index in HP, SSA/P, and TSA, in the whole (B) and individual parts (C). The central line is the arithmetic mean; error bars are \pm SD. (* P <0.05; ** P <0.01, Wilcoxon's rank-sum test). HP, hyperplastic polyp; SSA/P, sessile serrated adenoma/polyp; TSA, traditional serrated polyp.

middle zone, the rate of senescent cells in SSA/Ps was significantly higher than that in HPs, and the rate of senescent cells in TSAs was significantly higher than that in HPs. In the lower zone, the rate of senescent cells in SSA/Ps was significantly higher than that in HPs, and the rate of senescent cells in TSAs was significantly higher than in HPs. In the crypt as a whole, i.e. the lower, middle, and upper zones, there were significantly more senescent cells in SSA/Ps than in HPs, and significantly more senescent cells in TSAs than in SSA/Ps (2.37, 5.81, and 11.22% in HPs, SSA/Ps, and TSAs, respectively).

These data demonstrate that there were very few p16-positive senescent cells in the central bottom of the elongated

crypt in HPs; they were sparsely observed in the cleft of L- or T-shaped crypts in SSA/Ps, and were detected broadly across the crypt in TSAs. This suggests that there may be a difference in HP-SSA/P sequence and TSA progression in terms of senescence of the crypt epithelium.

Absence of p16-positive senescent cells co-expressed with Ki67-positive proliferating cells in L- and T-shaped crypts of SSAPs. We hypothesized that the sparse distribution of p16-positive senescent cells in the HP-SSA/P sequence may contribute to the distinctive morphology, such as the L- and T-shaped crypts of SSA/Ps. To verify this hypothesis, we

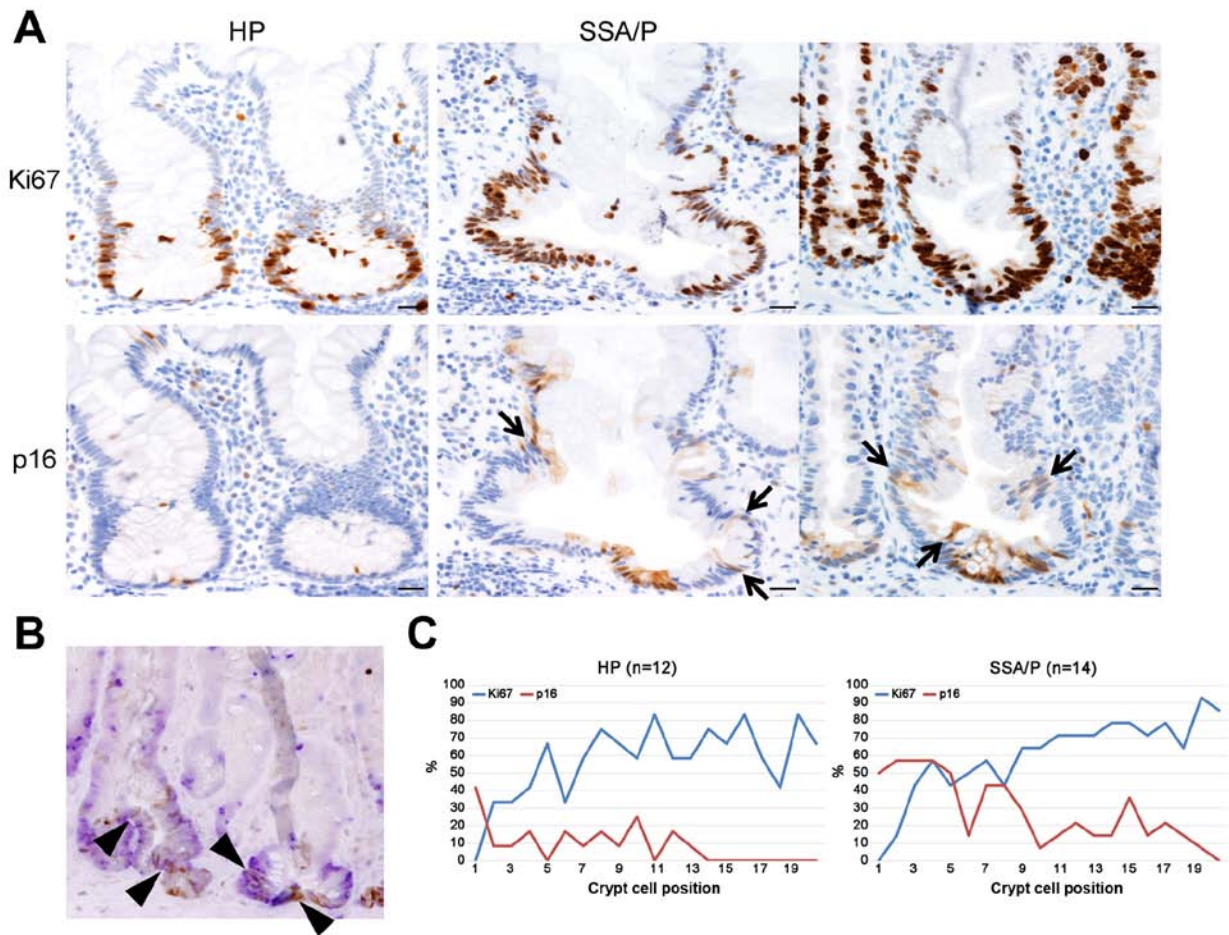


Figure 4. Distribution of Ki67-positive and p16-positive cells around the crypt (base) bottom. (A) Immunohistochemical expression of Ki67 (upper panels) and p16 (lower panels) at the serial section in HP and SSA/P. p16-positive cells at the cleft of the dividing crypt (arrows) (scale bars: 50 μ m). (B) Double-immunohistochemical staining for Ki67 (blue) and p16 (brown). Arrowheads indicate p16-positive cells localized at the crypt cleft. (C) Average cell positions of Ki67- (blue line) and p16- (red line) positive cells in HP and SSA/P. The crypt bottom means number '0'. HP, hyperplastic polyp; SSA/P, sessile serrated adenoma/polyp; TSA, traditional serrated polyp.

performed IHC in the serial section and performed double IHC for Ki67 and p16 in some crypts of SSA/P. In serial sections, Ki67- and p16-positive cells did not colocalize in the bottom of crypts in HPs or SSA/Ps (Fig. 4A). In HPs, a few p16-positive cells were found in the central of the crypt bottom, while Ki67-positive cells were distributed in the lower zone of the crypt, except for the central of the crypt bottom. In SSA/Ps, Ki67-positive cells were mainly found in the lower zone of the crypt and dilated crypts, although p16-positive cells were observed in the lower bottom of the cleft. These findings were confirmed using double IHC for Ki67 and p16 (Fig. 4B).

Next, we evaluated the overlap of Ki67- and p16-positive cells in the bottom and lower zones of the crypt in HPs and SSA/Ps by counting cells (Fig. 4C). In HPs, the majority of Ki67-positive cells were distinct from p16-positive cells in terms of their localizations. Most p16-positive cells were located immediately below the proliferation zone, marked by Ki67, and were expressed mainly in the bottom (base) of the crypt, which was defined as the +1 position. In SSA/Ps, the majority of Ki67-positive cells were also distinct from p16-positive cells in terms of their localizations; however, most p16-positive cells overlapped with Ki67-positive cells, and were expressed predominantly at the +2 to +8 positions.

These results suggest that sporadic cellular senescence may rearrange the distribution of proliferating cells, followed by elongation of the crypt during proliferation, which could induce distinctive architectural change around the bottom of the crypt in SSA/Ps.

Stromal Wnt5a-positive cells descend along the pericrypt and are located at the crypt cleft in SSA/Ps. We investigated whether Wnt5a is involved in the L- and T-shaped morphological changes in SSA/Ps; we performed IHC for Wnt5a in the same specimens investigated for Ki67 and p16 (HPs, n=20; SSA/Ps, n=40; TSAs, n=23). In HPs, Wnt5a-positive cells were observed in the stroma of the upper zone and immediately below the superficial epithelium, and were identified as myofibroblasts and lymphocytes (Fig. 5A). In SSA/Ps, Wnt5a-positive cells expanded from the upper to the middle zone of the crypt, laterally. To clarify the distribution of Wnt5a-positive cells in serrated lesions, we measured the number of positive cells per crypt, divided into the upper, middle, and lower zones, in HPs, SSA/Ps, and TSAs. The number of stromal Wnt5a-positive cells in SSA/Ps and TSAs was significantly higher than that in HPs in the upper and middle zones, but not in the lower zone (Fig. 5B). When we divided the upper zone

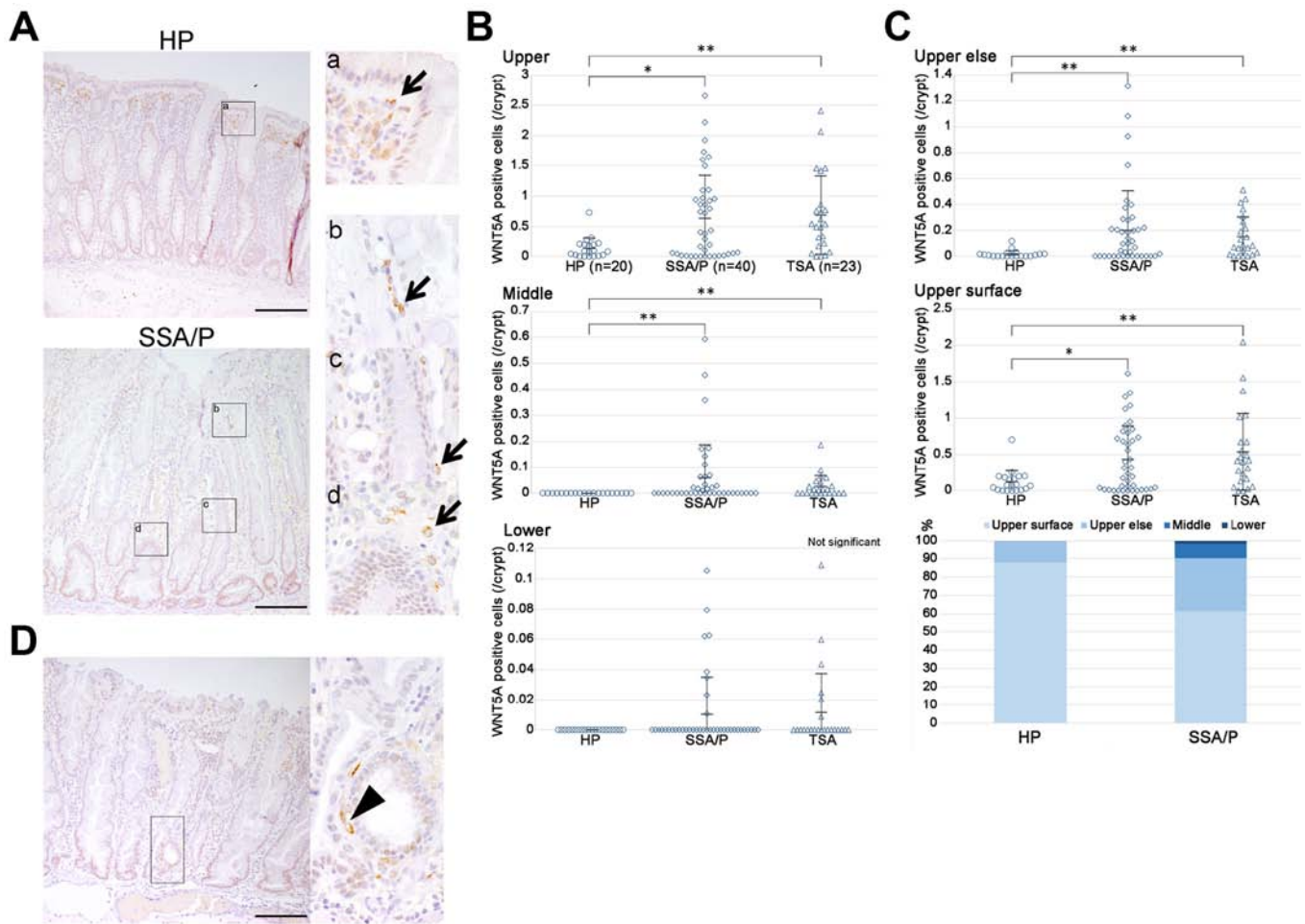


Figure 5. Wnt5a expression in HP, SSA/P, and TSA. (A, a-d) Representative images of immunohistochemical expression of Wnt5a in HP and SSA/P. Stromal Wnt5a-positive cells are localized along the pericrypt (arrows) (scale bars: 200 μ m). (B and C) Wnt5a-positive rates in HP, SSA/P, and TSA in individual parts. The central line is the arithmetic mean; error bars are \pm SD. ($P < 0.05$; $**P < 0.01$, Wilcoxon's rank-sum test). (D) Representative images of immunohistochemical expression of Wnt5a in the lower zone of SSA/P. Stromal Wnt5a-positive cells are localized around the crypt cleft (arrowhead) (scale bars: 200 μ m). HP, hyperplastic polyp; SSA/P, sessile serrated adenoma/polyp; TSA, traditional serrated polyp.

into 'upper else' and 'upper surface' areas (Fig. 2B), the difference in the number of stromal Wnt5a-positive cells was larger and more significant in 'upper else' area than 'upper surface' area between HPs and SSA/Ps (Fig. 5C). The difference was found not only in the number, but also in the distribution of these cells in HPs and SSA/Ps. These results indicated that stromal Wnt5a-positive cells may have migrated from the upper to middle zones in the HP-SSA/P sequence. Of note, some stromal Wnt5a-positive cells were found around clefts of the nascent front of crypts in SSA/Ps (Fig. 5D). This suggests that stromal Wnt5a-positive cells may be critical during the L- and T-shaped morphology changes in SSA/Ps.

Significant increases in intraepithelial lymphocytes in SSA/Ps. Thus, we evaluated IELs in the serrated precursor lesions, i.e., HPs and SSA/Ps (Fig. 6A). The mean number of IELs per crypt was 0.71 ± 0.56 and 1.83 ± 1.20 in HPs and SSA/Ps, respectively (Fig. 6B). The number of IELs in SSA/Ps was significantly increased as compared to HPs. This observation suggested that an increase in IELs was associated with the HP-SSA/P sequence as well as with the dysplasia-carcinoma sequence in the serrated pathway.

Discussion

In this study, we demonstrated that the number and distribution of epithelial proliferative (Ki67-positive) and senescent (p16-positive) cells contribute to distinctive morphology changes in the HP-SSA/P sequence of the serrated pathway. Furthermore, we showed that stromal Wnt5a-positive cells increase along the crypt elongation and branching, and the number of IELs increase in the HP-SSA/P sequence.

Previous studies have shown that the number and distribution of Ki67-positive cells differed between HPs and SSA/Ps, with a higher Ki67-positive rate and asymmetrical distribution in SSA/Ps (9). However, such differences were not confirmed in our study. This might be because 6/22 (27.3%) of HPs classified in our study were >10 mm, which are described as large hyperplastic polyp (LHPs), and have been considered to be synonymous with SSA/Ps in the WHO 2010 classification (Fig. 1B) (25-27). A recent study (28) supports our findings that there was no difference in Ki67 expression between HPs and SSA/Ps.

Our data suggested that p16-positive cells increased and expanded during the progression from HP to SSA/P in the

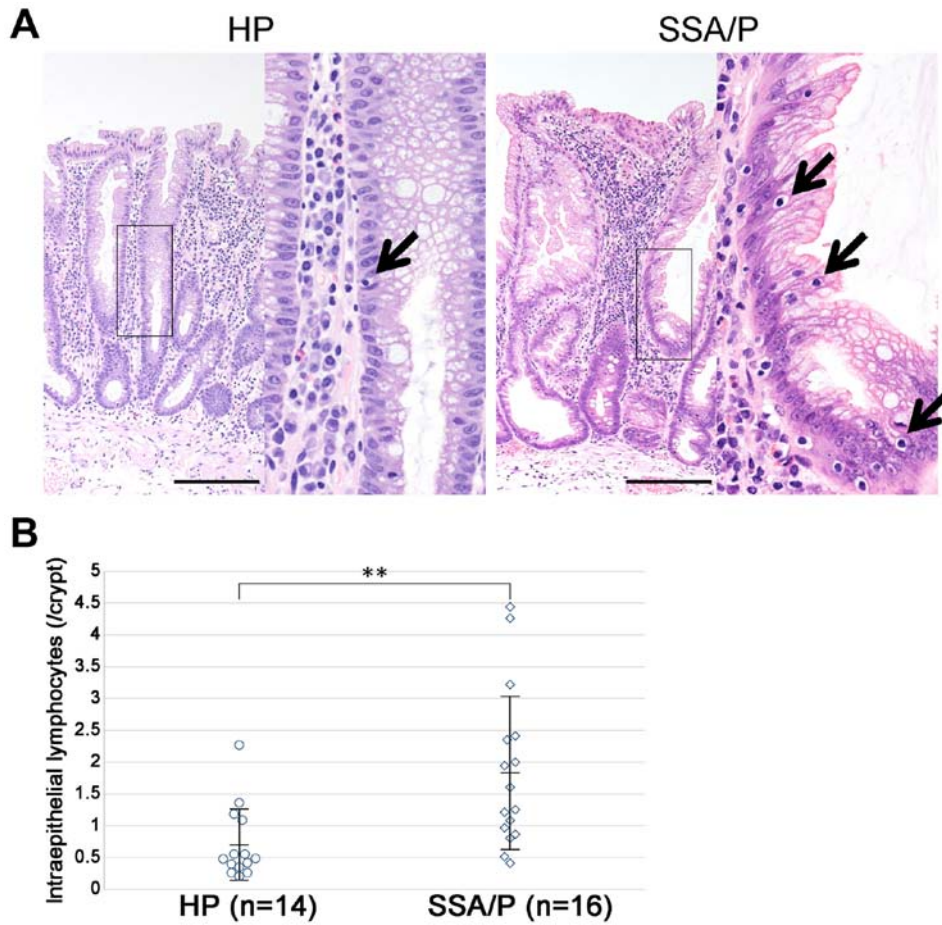


Figure 6. IELs in HP and SSA/P. (A) Representative images of IEL-enriched HP and SSA/P. Arrows indicate the intrusion of lymphocytes into crypt epithelium. (scale bars: 200 μ m). (B) The number of IELs in HP and SSA/P. The central line is the arithmetic mean; error bars are \pm SD. (** P <0.01, Wilcoxon's rank-sum test). IELs, intraepithelial lymphocytes; HP, hyperplastic polyp; SSA/P, sessile serrated adenoma/polyp; TSA, traditional serrated polyp.

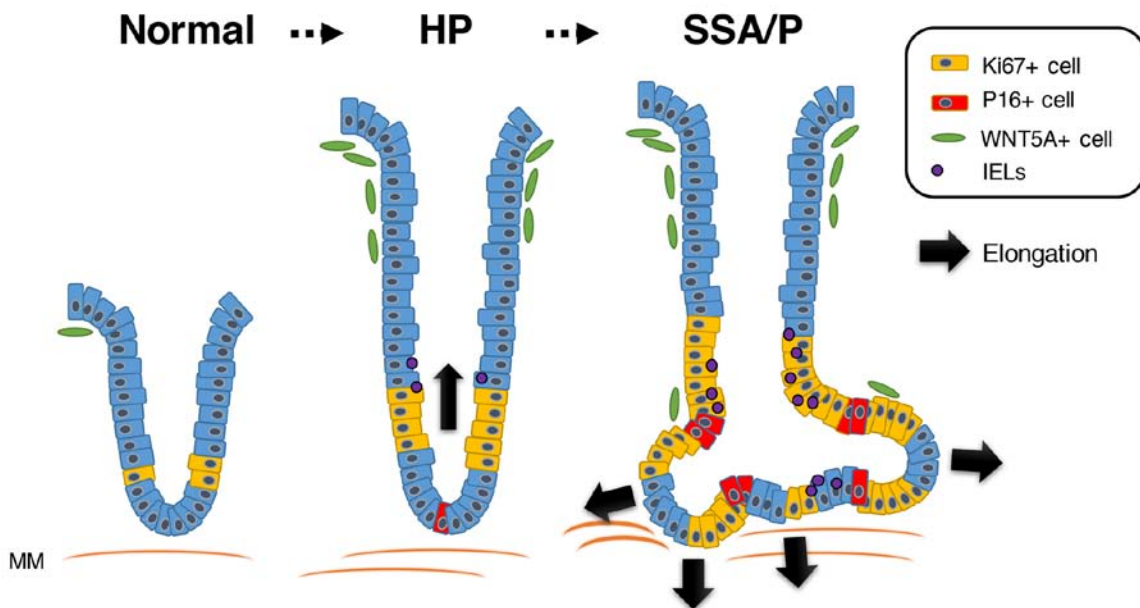


Figure 7. Schematic diagram of the proposed role of Ki67-, p16-, WNT5A-positive cells and IELs in the HP-SSA/P sequence, particularly the elongation of the branching crypt, such as L- and T-shaped crypts, in SSA/P. In HP, Ki67-positive proliferative cells increase and some p16-positive senescent cells, which arrest growth, appear in the bottom of the crypt (base), thus leading to crypt elongation. Furthermore, stromal WNT5A-positive cells increase in the upper zone, and several IELs are seen. In SSA/P, p16-positive senescent cells increase and have a patchy distribution in the crypt epithelium in the lower zone, and the branching crypt elongates, which act as fixed supports. WNT5A-positive cells descend along the pericrypt to the middle zone and some cells are located in the cleft of the elongating crypts. IELs increase in SSA/P. IELs, intraepithelial lymphocytes; MM, muscularis mucosa; HP, hyperplastic polyp; SSA/P, sessile serrated adenoma/polyp; TSA, traditional serrated polyp.

HP-SSA/P sequence. In human serrated lesions, oncogene-induced senescence is induced by initiating BRAF mutations, which lead to premalignant lesions, with upregulation of p16 and growth limitation by the senescence barrier (18). We demonstrated that there were few p16-positive senescent cells in the bottom of crypts in HPs, although there were no cells in normal crypts. Furthermore, in SSA/Ps, p16-positive senescent cells were distributed mainly in a patchy fashion and at the clefting point. Noteworthy, those p16-positive cells did not co-localize with Ki67-positive proliferating cells. Kreigl *et al* (18) showed that p16 and Ki67 expression were mutually exclusive in premalignant lesions, such as serrated polyps; however, the distribution of expression of both these proteins was unclear in SSA/Ps. Our results indicated that a patchy distribution of senescent and proliferating cells may distinguish the morphology in the HP-SSA/P sequence (Fig. 7).

Microscopically, in contrast to HPs and SSA/Ps, TSAs are protuberant, exophytic, and villous, and have many ectopic crypt foci, which is the hallmark of TSA lesions (29). We analyzed the Ki67-proliferative and p16-senescent cells in TSAs, as well as in HPs and SSA/Ps. The distribution of both Ki67- and p16-positive cells was broadly expanded throughout the crypt and could clearly distinguish TSAs from HPs and SSA/Ps. Furthermore, our data and those of previous studies demonstrated that TSAs usually develop in the left-sided colon, while SSA/Ps develop in the right-sided colon. This suggests that TSAs may not be related to HPs and SSA/Ps in terms of histological, molecular, and territorial pathogenesis.

It has been reported that stromal Wnt5a enhances transforming growth factor- β signaling to reduce epithelial proliferation and cause clefting of epithelial channels, and clefting modifies the polarization of highly proliferative crypt structures at wound margins, allowing them to branch into new crypt units in the regeneration of crypts in mice (20). Of note, this phenomenon supports our finding that stromal Wnt5a-positive cells were localized near the cleft of crypts in human SSA/Ps. This indicates a morphological similarity between regenerative branching and branching of crypts in SSA/Ps. Furthermore, our results demonstrated that the number of IELs in SSA/Ps was significantly increased as compared with that in HPs, suggesting that inflammation may accelerate the morphological changes in SSA/Ps. Hence, we hypothesized that the distinctive morphological changes in SSA/Ps might be caused by reactive changes, rather than by neoplastic changes, and SSA/Ps with dysplasia may demonstrate distinct neoplastic changes. Furthermore, histological and molecular studies are necessary to clarify the pathogenesis of SSA/Ps that are distinguished by the presence of dysplasia.

Recently, noncanonical Wnt signaling pathway, such as WNT5A and WNT3A, has been implicated in the regulation of mesenchymal stem cell differentiation, including adipogenic differentiation (30). By WNT5A activation, human adipose-derived stem cells can differentiate neurogenic cells in a 3D microfluidic culture systems (31), thus suggesting that WNT5A activation might be a key gene in neural differentiation of mesenchymal stem cells (32). In gastrointestinal polyps, primary neurogenic polyps are frequently observed (33). However, the pathogenesis remains unclear. WNT5A may be associated with the development of the neurogenic gastrointes-

tinal polyps on not only surrounding tumor microenvironment but also the stem cell differentiation.

Taken together, this study demonstrates evidence that HP elongates and branches, based on the increase and patchy distribution of senescent and proliferative cells, along with activation of stromal and inflammatory cells, which contributes to producing the L- and/or T-shaped crypts that are distinctive in SSA/Ps. Our findings may facilitate understanding and improve therapy of serrated lesions.

Acknowledgements

We thank Kyoko Takahashi, Ayako Suga, Masayoshi Shimizu, and Reiko Kitazumi for assistance with the experiments. This work was supported by grants from the Ministry of Education, Culture, Sports, Science, and Technology of Japan: grant nos. 15K11289 and 26430111 (A.H. and H.T., respectively).

References

1. Snover D, Ahnen DJ, Burt RW and Odze RD: Serrated polyps of the colon and rectum and serrated polyposis. In: WHO Classification of Tumours of the Digestive System. Vol 3. 4th edition. Bosman FT, Carneiro F, Hruban RH and Theise ND (eds). IARC, Lyon, France, pp160-165, 2010.
2. Snover DC: Update on the serrated pathway to colorectal carcinoma. *Hum Pathol* 42: 1-10, 2011.
3. Chan TL, Zhao W, Leung SY and Yuen ST: Cancer Genome Project: BRAF and KRAS mutations in colorectal hyperplastic polyps and serrated adenomas. *Cancer Res* 63: 4878-4881, 2003.
4. Iino H, Jass JR, Simms LA, Young J, Leggett B, Ajioka Y and Watanabe H: DNA microsatellite instability in hyperplastic polyps, serrated adenomas, and mixed polyps: A mild mutator pathway for colorectal cancer? *J Clin Pathol* 52: 5-9, 1999.
5. Park SJ, Rashid A, Lee JH, Kim SG, Hamilton SR and Wu TT: Frequent CpG island methylation in serrated adenomas of the colorectum. *Am J Pathol* 162: 815-822, 2003.
6. Spring KJ, Zhao ZZ, Karamatic R, Walsh MD, Whitehall VL, Pike T, Simms LA, Young J, James M, Montgomery GW, *et al*: High prevalence of sessile serrated adenomas with BRAF mutations: A prospective study of patients undergoing colonoscopy. *Gastroenterology* 131: 1400-1407, 2006.
7. Yang S, Farraye FA, Mack C, Posnik O and O'Brien MJ: BRAF and KRAS mutations in hyperplastic polyps and serrated adenomas of the colorectum: Relationship to histology and CpG island methylation status. *Am J Surg Pathol* 28: 1452-1459, 2004.
8. Carr NJ, Mahajan H, Tan KL, Hawkins NJ and Ward RL: Serrated and non-serrated polyps of the colorectum: Their prevalence in an unselected case series and correlation of BRAF mutation analysis with the diagnosis of sessile serrated adenoma. *J Clin Pathol* 62: 516-518, 2009.
9. Fujimori Y, Fujimori T, Imura J, Sugai T, Yao T, Wada R, Ajioka Y and Ohkura Y: An assessment of the diagnostic criteria for sessile serrated adenoma/polyps: SSA/Ps using image processing software analysis for Ki67 immunohistochemistry. *Diagn Pathol* 7: 59, 2012.
10. Higuchi T, Sugihara K and Jass JR: Demographic and pathological characteristics of serrated polyps of colorectum. *Histopathology* 47: 32-40, 2005.
11. O'Brien MJ, Yang S, Mack C, Xu H, Huang CS, Mulcahy E, Amoroso M and Farraye FA: Comparison of microsatellite instability, CpG island methylation phenotype, BRAF and KRAS status in serrated polyps and traditional adenomas indicates separate pathways to distinct colorectal carcinoma end points. *Am J Surg Pathol* 30: 1491-1501, 2006.
12. Chetty R, Hafezi-Bakhtiari S, Serra S, Colling R and Wang LM: Traditional serrated adenomas (TSAs) admixed with other serrated (so-called precursor) polyps and conventional adenomas: A frequent occurrence. *J Clin Pathol* 68: 270-273, 2015.
13. Schmitt CA: Cellular senescence and cancer treatment. *Biochim Biophys Acta* 1775: 5-20, 2007.
14. Collado M, Blasco MA and Serrano M: Cellular senescence in cancer and aging. *Cell* 130: 223-233, 2007.

15. Campisi J and d'Adda di Fagagna F: Cellular senescence: When bad things happen to good cells. *Nat Rev Mol Cell Biol* 8: 729-740, 2007.
16. Gutierrez-Reyes G, del Carmen Garcia de Leon M, Varela-Fascinetto G, Valencia P, Pérez Tamayo R, Rosado CG, Labonne BF, Rochilin NM, Garcia RM, Valadez JA, *et al*: Cellular senescence in livers from children with end stage liver disease. *PLoS One* 5: e10231, 2010.
17. Dankort D, Filenova E, Collado M, Serrano M, Jones K and McMahon M: A new mouse model to explore the initiation, progression, and therapy of BRAFV600E-induced lung tumors. *Genes Dev* 21: 379-384, 2007.
18. Kriegl L, Neumann J, Vieth M, Greten FR, Reu S, Jung A and Kirchner T: Up and downregulation of p16(Ink4a) expression in BRAF-mutated polyps/adenomas indicates a senescence barrier in the serrated route to colon cancer. *Mod Pathol* 24: 1015-1022, 2011.
19. Shida Y, Ichikawa K, Fujimori T, Fujimori Y, Tomita S, Fujii T, Sano Y, Oda Y, Goto H, Ohta A, *et al*: Differentiation between sessile serrated adenoma/polyp and non-sessile serrated adenoma/polyp in large hyperplastic polyp: A Japanese collaborative study. *Mol Clin Oncol* 1: 53-58, 2013.
20. Miyoshi H, Ajima R, Luo CT, Yamaguchi TP and Stappenbeck TS: Wnt5a potentiates TGF- β signaling to promote colonic crypt regeneration after tissue injury. *Science* 338: 108-113, 2012.
21. Powell DW, Adegboyega PA, Di Mari JF and Mifflin RC: Epithelial cells and their neighbors I. Role of intestinal myofibroblasts in development, repair, and cancer. *Am J Physiol Gastrointest Liver Physiol* 289: G2-G7, 2005.
22. Gregorieff A, Pinto D, Begthel H, Destree O, Kielman M and Clevers H: Expression pattern of Wnt signaling components in the adult intestine. *Gastroenterology* 129: 626-638, 2005.
23. Rau TT, Atreya R, Aust D, Baretton G, Eck M, Erlenbach-Wünsch K, Hartmann A, Lugli A, Stöhr R, Vieth M, *et al*: Inflammatory response in serrated precursor lesions of the colon classified according to WHO entities, clinical parameters and phenotype-genotype correlation. *J Pathol Clin Res* 2: 113-124, 2016.
24. Tanaka K, Tomita H, Hisamatsu K, Nakashima T, Hatano Y, Sasaki Y, Osada S, Tanaka T, Miyazaki T, Yoshida K, *et al*: ALDH1A1-overexpressing cells are differentiated cells but not cancer stem or progenitor cells in human hepatocellular carcinoma. *Oncotarget* 6: 24722-24732, 2015.
25. Jass JR: Serrated adenoma of the colorectum and the DNA-methylator phenotype. *Nat Clin Pract Oncol* 2: 398-405, 2005.
26. Warner AS, Glick ME and Fogt F: Multiple large hyperplastic polyps of the colon coincident with adenocarcinoma. *Am J Gastroenterol* 89: 123-125, 1994.
27. Tinmouth J, Henry P, Hsieh E, Baxter NN, Hilsden RJ, Elizabeth McGregor S, Paszat LF, Ruco A, Saskin R, Schell AJ, *et al*: Sessile serrated polyps at screening colonoscopy: Have they been under diagnosed? *Am J Gastroenterol* 109: 1698-1704, 2014.
28. Dayi N, Baba HA, Schmid KW and Schmitz KJ: Increased expression of α -methylacyl-coenzyme A racemase (AMACR; p504s) and p16 in distal hyperplastic polyps. *Diagn Pathol* 8: 178, 2013.
29. Chetty R: Traditional serrated adenoma (TSA): Morphological questions, queries and quandaries. *J Clin Pathol* 69: 6-11, 2016.
30. Yuan Z, Li Q, Luo S, Liu Z, Luo D, Zhang B, Zhang D, Rao P and Xiao J: PPAR γ and Wnt signaling in adipogenic and osteogenic differentiation of mesenchymal stem cells. *Curr Stem Cell Res Ther* 11: 216-225, 2016.
31. Choi J, Kim S, Jung J, Lim Y, Kang K, Park S and Kang S: Wnt5a-mediating neurogenesis of human adipose tissue-derived stem cells in a 3D microfluidic cell culture system. *Biomaterials* 32: 7013-7022, 2011.
32. Cardozo AJ, Gómez DE and Argibay PF: Neurogenic differentiation of human adipose-derived stem cells: Relevance of different signaling molecules, transcription factors, and key marker genes. *Gene* 511: 427-436, 2012.
33. Hechtman JF and Harpaz N: Neurogenic polyps of the gastrointestinal tract: A clinicopathologic review with emphasis on differential diagnosis and syndromic associations. *Arch Pathol Lab Med* 139: 133-139, 2015.